JACS
JOURNAL OF THE AMERICAN CHEMICAL SOCIETY

ARTICLE

pubs.acs.org/JACS

Activation Energies for the Rate-Limiting Step in Water Photooxidation by Nanostructured α-Fe_2O_3 and TiO_2

Alexander J. Cowan,[†] Christopher J. Barnett,[†] Stephanie R. Pendlebury,[†] Monica Barroso,[†] Kevin Sivula,[‡] Michael Grätzel,[‡] James R. Durrant,[†] and David R. Klug*[,†]

[†]Chemistry Department, Imperial College London, South Kensington Campus, SW7 2AZ, U.K.

[‡]Institut des Sciences et Ingénierie Chimiques, Ecole Polytechnique Fédérale de Lausanne, CH-1015 Lausanne, Switzerland;

Supporting Information

ABSTRACT: Competition between charge recombination and the forward reactions required for water splitting limits the efficiency of metal-oxide photocatalysts. A key requirement for the photochemical oxidation of water on both nanostructured α-Fe_2O_3 and TiO_2 is the generation of photoholes with lifetimes on the order of milliseconds to seconds. Here we use transient absorption spectroscopy to directly probe the long-lived holes on both nc-TiO_2 and α-Fe_2O_3 in complete PEC cells, and we investigate the factors controlling this slow hole decay, which can be described as the rate-limiting step in water oxidation. In both cases this rate-limiting step is tentatively assigned to the hole transfer from the metal oxide to a surface-bound water species. We demonstrate that one reason for the slow hole transfer on α-Fe_2O_3 is the presence of a significant thermal barrier, the magnitude of which is found to be independent of the applied bias at the potentials examined. This is in contrast to nanocrystalline nc-TiO_2, where no distinct thermal barrier to hole transfer is observed.

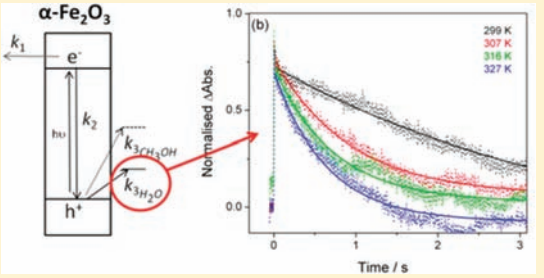

INTRODUCTION

Environmental concerns have led to renewed interest in the production of hydrogen by photochemical routes. Since the pioneering works on TiO_2 by Boddy[1] and Fujishima and Honda,[2] there have been significant advances in the development of both new materials and architectures for existing materials, and details of the current benchmark materials can be found in several recent reviews.[3,4] Despite these advances, there are currently no commercially viable materials that are able to maintain the proposed minimum 10% requirement for solar energy to hydrogen fuel efficiency.[5] A key issue hindering the rational design of new materials is the very limited data available to elucidate the mechanisms of the multistep oxidation of water by existing materials.

As part of a program that aims to increase our understanding of the mechanistic constraints that lead to low efficiencies for photochemical water oxidation by metal oxide systems, we are studying the mechanism of photochemical water oxidation in two well-known metal oxide photocatalysts, nanocrystalline (nc) TiO_2 and nanostructured hematite (α-Fe_2O_3). The wide band gap of TiO_2 (~3.2 eV) limits its photoactivity to the UV region of the solar spectrum, and relatively low quantum yields are often reported for photochemical water splitting over TiO_2, which further limits its efficiency.[6] Despite this, there is still intense interest in this material for both light-driven water splitting and organic degradation, and numerous studies have aimed to enhance the efficiency of this material, primarily through visible light sensitization.[7−9] The factors controlling electron transport and recombination in nc-TiO_2 have been extensively studied due to the use of this material in dye-sensitized solar cells,[10,11] and the relatively well-characterized nature of nc-TiO_2 makes it an ideal model for mechanistic research.

Hematite (α-Fe_2O_3) has been proposed to be one of the most promising photoanode materials for use in a photoelectrochemical (PEC) cell for water splitting.[12] It has a band gap of ~2.0−2.2 eV, allowing it to absorb a significant portion of the solar spectrum, and has a valence band edge that is at a suitable energy for water oxidation. The conduction band edge of α-Fe_2O_3 is below that of the energy required for H_2 evolution, leading to the requirement of an external bias for H_2 production; however when used in a tandem cell[13] setup, it has been estimated that a solar to chemical energy conversion efficiency of 20% could be achieved.[14] Despite this current benchmark α-Fe_2O_3 photoanodes would achieve significantly lower conversion efficiencies in an appropriate tandem cell, indicating that there is still considerable scope for further improvement of this material.[15] The relatively long light penetration depth (ca. 100 nm with λ = 500 nm)[16] combined with a hole diffusion length that has been estimated to be between 2 and 20 nm[17,18] has been proposed to be one of the key loss pathways in α-Fe_2O_3, as photoholes generated deep within the material are unable to reach the surface before recombination occurs. It has also been proposed that a low rate constant for the oxidation of water by

Received: January 26, 2011
Published: May 09, 2011

surface-trapped holes is a significant issue on α-Fe_2O_3 photoelectrodes.[17] There have been a range of nanostructured materials prepared including nanotubes,[19] platelets,[20] and dendritic structures.[12] The dendritic α-Fe_2O_3 films prepared by atmospheric pressure chemical vapor deposition (APCVD) were found to give increased plateau photocurrents for water oxidation due to the generation of photoholes at short distances from the semiconductor liquid interface. Further material modifications including the addition of Si dopants to enhance diffusion lengths, a cobalt cocatalyst to aid hole accumulation, and a thin insulating SiO_2 layer at the α-Fe_2O_3/FTO interface increased the efficiency of the material, and an incident to photon current efficiency of 42% was reported (370 nm excitation, α-Fe_2O_3 at 1.23 V vs RHE, AM 1.5).[12] Nanostructuring of α-Fe_2O_3 has significantly improved the plateau photocurrents; however a further limiting factor in the use of α-Fe_2O_3 has been the requirement of a relatively large anodic bias (∼0.4 V vs the flat band potential) for water oxidation to occur.[14] It has been proposed that the large onset potential for water oxidation is associated with the slow kinetics of the hole reaction with water, as surface recombination of photoholes is expected to be a significant loss pathway in α-Fe_2O_3. The addition of either a cobalt catalyst[12,21] or an IrO_2 catalyst[15] to the α-Fe_2O_3 surface causes not only an increase in the plateau photocurrent but also a cathodic shift of between 350 and 200 mV to the onset photocurrents compared to the untreated Fe_2O_3 films, underlining the significance of understanding the kinetics of the hole reaction with water.

Transient absorption spectroscopy (TAS) can be used for the detection of short-lived intermediates following the excitation of a photocatalyst with a short pulse of light. TAS experiments on nc-TiO_2 have demonstrated that trapping of holes and electrons can occur on nc-TiO_2 in <200 fs and 500 ps, respectively.[22,23] The TAS spectra of trapped photoholes and electrons on nc-TiO_2 have been reported by several different groups, and the rates of recombination, which is controlled by the electron density of the material, have been investigated.[24−27] On nc-TiO_2 photoanodes at pH 12.6 the required photohole lifetime for water oxidation has been estimated to be ∼30 ms, while at neutral pH's in the presence of an electron scavenger a hole lifetime of 0.2 s has been reported.[27,28] The requirement of such long-lived photoholes for the oxidation of water on nc-TiO_2 enables significant levels of electron−hole recombination to occur prior to the hole transfer into solution. It is the balance between the rates of electron hole recombination, hole transfer into solution, and electron transport that is key in determining the efficiency of the photoanode.

TAS has been recently used to study the dynamics of photogenerated holes in nanocrystalline α-Fe_2O_3 electrodes. In the absence of an applied bias fast (μs−ms) electron−hole recombination occurs. When the α-Fe_2O_3 film was held at a positive potential, a long-lived transient absorption signal at 580 nm was observed.[29] Under conditions where water splitting occurs the photohole was found to have a lifetime of ∼3 s, indicating that the oxidation of water on α-Fe_2O_3 requires extremely long-lived holes and that the decay of the holes on this time scale was due to slow hole transfer kinetics. This report demonstrates that TAS can be used to directly follow the photohole dynamics and that on this material the requirement for such long-lived holes is likely to be one of the key factors controlling the efficiency of α-Fe_2O_3 photoanodes.

By studying the hole reaction kinetics on nc-TiO_2 and α-Fe_2O_3 within a complete photoelectrochemical cell we can improve our understanding of the fundamental factors behind the reported efficiencies of these materials. In both materials the rate-limiting step in the water oxidation is the very slow hole reaction that occurs on the ms−s time scale. TAS allows us to directly probe this step, and we have used variable-temperature experiments to measure the activation energies for this rate-limiting step, providing insights into the potential thermal barriers controlling the reported reaction rates.

EXPERIMENTAL SECTION

A TiO_2 colloid paste (12.5 wt % anatase TiO_2 particles and 6.2 wt % Carbowax 20000) was prepared in a manner previously described to produce TiO_2 particles with an average diameter of 15 nm.[30] The colloid paste was spread onto the surface of the substrate FTO glass (TEC-15, Hartford glass) using a K-bar (#2, RK print coat instruments) and dried in the air, then calcined at 450 °C for 30 min. The thickness of the resultant film was measured with a profilometer (Alpha-Step 200, Tencor Instruments) and found to be ∼1 μm. The α-Fe_2O_3 films used in our study were prepared by atmospheric pressure chemical vapor deposition and have a dendritic nanoporous structure; the films studied are undoped, and the method of their production is described elsewhere.[12] In order to minimize errors resulting from slight variations in the material preparation procedure, all data presented are from a single α-Fe_2O_3 electrode. Solutions of 0.5 M $NaClO_4$ and 0.05 M NaOH (Sigma Aldrich) were prepared from Milli-Q-Water (Millipore Corp, 18.2 MΩ cm at 298 K) and degassed with argon (BOC, Pureshield grade). The electrolyte composition was chosen to match that used in a previous TAS study of nc-TiO_2 electrodes,[28] and it is also suitable for the stable operation of α-Fe_2O_3 electrodes. Methanol (Aldrich, spectrophotometric grade) was used as received.

Variable-temperature transient measurements were carried out in custom-made Teflon-lined aluminum cells with two borosilicate glass windows containing the semiconductor photoanode, a Pt counter electrode, and a Ag/AgCl reference electrode (3.5 M KCl). The photoanodes were mounted with the substrate facing the excitation source (SE). Experiments were carried out using a Ministat 251 (Thompson Electrochemical). The cell temperature was controlled by resistive heaters on the cell body and a Pt resistance thermometer, which were linked to a PID controller. The electrolyte temperature was measured prior and post transient measurements and found to be stable in all cases to ±0.2 K. The effect of temperature on the reference electrode was calibrated by the use of the reported temperature coefficients,[31] and all potentials reported are equivalent to those versus Ag/AgCl at 298 K unless otherwise stated.

The TAS experiment has been described in detail elsewhere.[28] Briefly the sample is excited by a third harmonic of a Nd:YAG laser (Continuum, Surelite I-10, 355 nm, 6 ns pulse width). Laser intensities reported have been corrected for losses occurring from the cell front window and the FTO substrate. A 75 W Xe lamp is used as the probe beam with monochromators both before and after the sample employed, and the transmitted light level is measured with time following the UV excitation of the sample by a Si PIN photodiode (Hamamatsu). The variable-temperature TAS data are the result of averaging between 300 and 1000 laser shots at either 0.18 Hz (Fe_2O_3) or 0.33 Hz (TiO_2).

RESULTS

Current−voltage curves for nc-TiO_2 and α-Fe_2O_3 films in 0.5 M $NaClO_4$/0.05 M NaOH are shown in Figure 1. In agreement with previous reports the strong photocurrent from α-Fe_2O_3 observed at potentials positive of 0 V vs Ag/AgCl is assigned to the photochemical oxidation of water, Figure 1a.[12] Likewise the photocurrent observed at potentials positive of −0.8 V vs Ag/AgCl

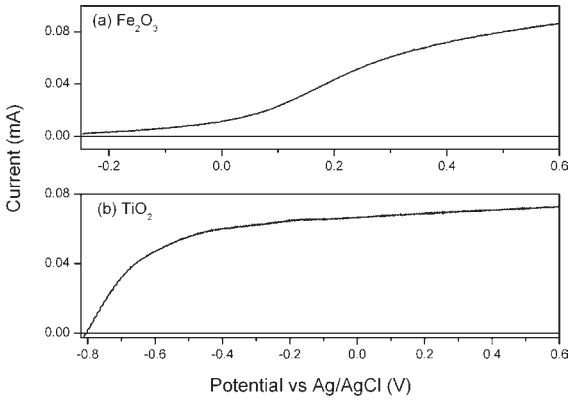

Figure 1. Photoelectrochemical response of (a) CVD-Fe_2O_3 and (b) nc-TiO_2 photoelectrodes illuminated by 355 nm light (75 W Xe lamp) in 0.05 M NaOH/0.5 M $NaClO_4$ electrolyte.

from nc-TiO_2 is assigned to photochemical oxidation of water, Figure 1b.[32] By carrying out TAS experiments on the same cells at potentials positive of the photocurrent onset, it is possible to follow the kinetics of the electrons and holes during water splitting.[28] It has been recently reported that the surface-trapped photoholes on α-Fe_2O_3 that are active for oxidation reactions have an absorption at 580 nm. Under conditions where water oxidation occurs the photohole decays very slowly, and this has been proposed to be due to a slow hole transfer step during the water oxidation ($k_{obs} \approx 0.3\ s^{-1}$).[29] Slow surface oxidation kinetics have been advocated to be a key factor in the requirement of a ~200−300 mV versus the flat band potential for water oxidation to occur on α-Fe_2O_3.[15,17]

Temperature Dependence of the Rate-Limiting Step in α-Fe_2O_3. It has been proposed that the hole on α-Fe_2O_3 has Fe(IV) character,[17] leading to retarded rates of hole transfer to water when compared to transfer from O 2p orbitals; however the fundamental causes of the slow surface oxidation kinetics on α-Fe_2O_3 are not fully understood and have not been demonstrated experimentally. TAS spectroscopy allows us to directly probe the hole kinetics, and we are able to obtain detailed information about the rate-limiting step in the water splitting cell. A typical TAS spectrum recorded following the UV excitation (355 nm, 300 $\mu J\ cm^{-2}$) of an α-Fe_2O_3 photoanode at 445 mV (vs Ag/AgCl) at room temperature in 0.05 M NaOH/0.5 M $NaClO_4$ is shown in Figure 2a. At >10 ms a very long-lived transient absorption band from ~520 to 700 nm is observed. The slow decay (milliseconds to seconds) of the transient signals between 580 and 700 nm is fitted to a single-exponential decay function, and at 299 K the hole decay rate is found to be $k_{obs} = 3.8 \times 10^{-1}\ s^{-1}$ (580 nm), Figure 2b. By comparison to previous reports the transient signals between 580 and 700 nm are assigned to surface-trapped photoholes.[29] Detailed analysis of the transient absorption spectrum (Figure S3) shows that there is a faster decay at wavelengths below 550 nm, a region where we are heavily overlapped with the ground-state absorption spectrum of α-Fe_2O_3, and this is proposed to be due to a change in ground-state character. Importantly the observation that photohole decay between 580 and 700 nm can be fitted to a single-exponential decay function indicates that a single decay pathway dominates on these time scales. The rate of photohole decay is temperature dependent, and an Arrhenius plot of the temperature dependence yields an activation energy of 0.45 ± 0.04 eV,

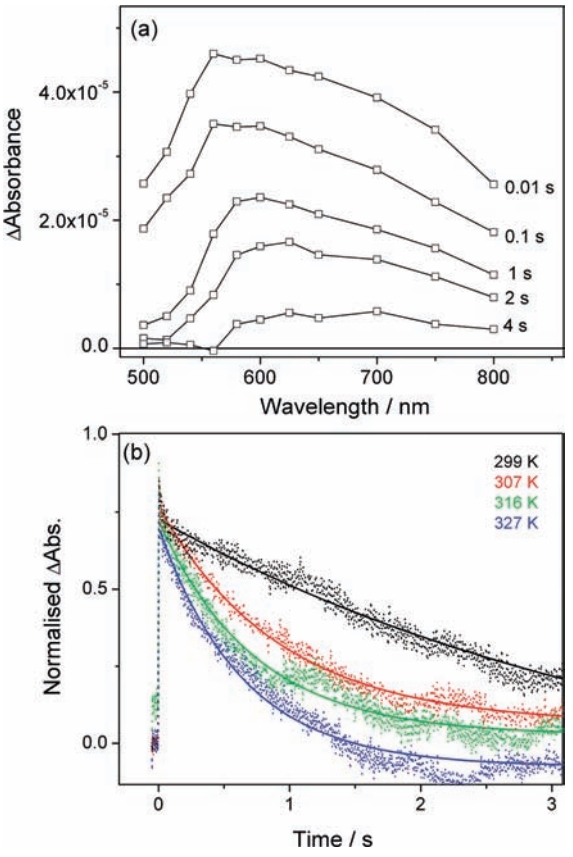

Figure 2. (a) Transient absorption spectrum of the photohole recorded following the UV excitation (355 nm, 300 $\mu J\ cm^{-2}$, 0.18 Hz) of CVD-Fe_2O_3 held at 445 mV vs Ag/AgCl reference electrode. (b) TAS decay traces of the photohole at different temperatures fitted to single-exponential functions. The hole decay was recorded at 580 nm following the UV excitation of CVD-Fe_2O_3 film held at a constant applied potential (equivalent to 445 mV vs Ag/AgCl at 299 K).

Figure 3. Activation energies of similar magnitudes (0.2−0.7 eV) for the electrical conductivity have been previously reported by several groups on α-Fe_2O_3.[33,34] Transient photocurrent measurements, details of which can be found in the SI, demonstrate that in this study we are not probing this temperature dependence of electron transport, as under the conditions employed electron transport is occurring on a markedly faster time scale (μs−ms) than the slow hole reaction that we are probing. The temperature dependence of the photohole decay rate in the presence of methanol has also been examined (α-Fe_2O_3 held at 445 mV (vs Ag/AgCl) in 0.05 M NaOH/0.5 M $NaClO_4$ and 10% methanol, 355 nm, 300 $\mu J\ cm^{-2}$ excitation). In agreement with previous reports we find that the photohole decays at a faster rate in the presence of methanol, $k_{obs} = 2.7\ s^{-1}$ (299 K).[29] The activation energy for the photohole decay is found to be considerably lower in the presence of methanol (0.13 ± 0.04 eV), Figure 3c. The dependence of the slow hole decay rate and its associated activation energy on the nature of the surface species leads us to tentatively assign the rate-limiting step probed to a hole transfer step from the α-Fe_2O_3 to solution or to a surface-bound species, the nature of which is discussed further below. The decreased activation barrier to this step during methanol oxidation correlates with the increased rate of hole decay and with the higher thermodynamic driving force for the

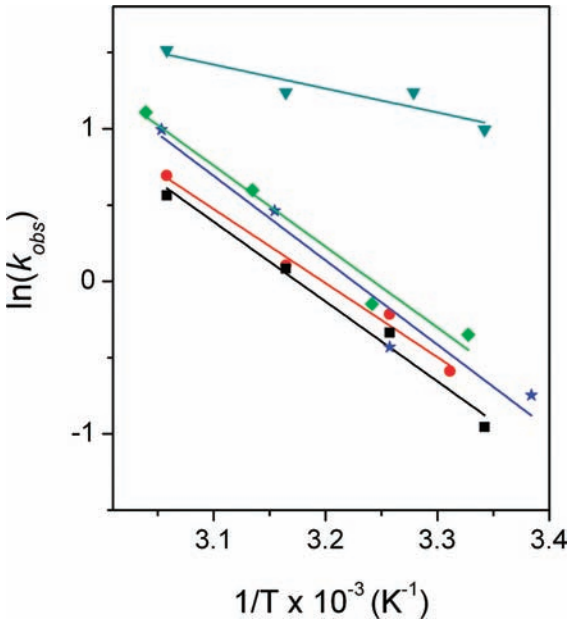

Figure 3. Arrhenius plots of the hole decay during the photoxidation of water on CVD-Fe_2O_3 held at 545 mV (green diamonds), 445 mV (black squares), 345 mV (blue stars), and 245 mV (red circles) vs Ag/AgCl at 299 K in 0.05 M NaOH/0.5 M $NaClO_4$. Arrhenius plot of the hole decay during the photoxidation of methanol (cyan triangles) on CVD-Fe_2O_3 held at 445 mV (vs Ag/AgCl at 299 K) in 0.05 M NaOH/0.5 M $NaClO_4$ with 10% methanol. All hole decay rates were recorded by measuring the TAS signal at 580 nm following the UV excitation (355 nm, 300 μJ cm^{-2}, 0.18 Hz).

Scheme 1. Kinetic Scheme for the Photocatalytic Oxidation of Water on nc-TiO_2 or α-Fe_2O_3[a]

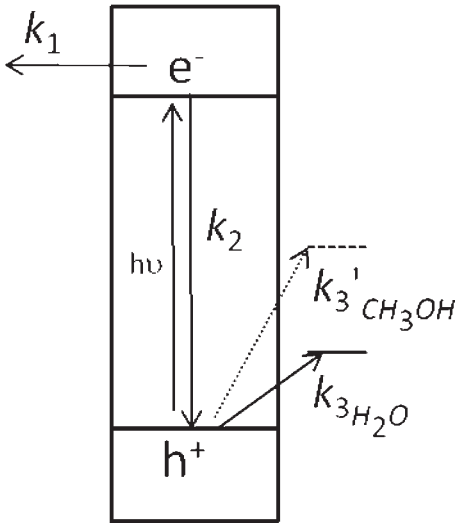

[a] The balance between the rates of electron/hole recombination (k_2), electron transport and withdrawal (k_1), and hole reaction (k_3) controls the overall efficiency of the process. We tentatively assign the rate-limiting step to a terminal hole transfer (k_3). Rates shown as individual steps may occur by multiple steps.

oxidation of methanol compared to the oxidation of water, Scheme 1.

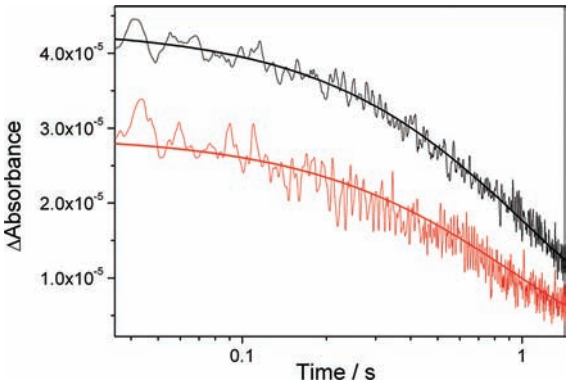

Figure 4. TAS decay traces of the photohole probed at 580 nm following the UV excitation of CVD-Fe_2O_3 film held at a constant applied potential of 445 mV (black trace) and 245 mV vs Ag/AgCl (red trace).

Role of Applied Bias on the Fe_2O_3 Hole Activation Energy. The requirement of a relatively large anodic bias for water oxidation to occur on α-Fe_2O_3 is a significant drawback, as it requires an energy input into the system. It is therefore important to understand the factors behind the requirement for this bias. The effect of the applied bias to the rate of photochemical reactions on the nanostructured electrodes used in this study is examined by measuring the rate of photohole decay on α-Fe_2O_3 during water oxidation at three further potentials that are significantly positive of the photocurrent onset potential (+245, +345, and +545 mV vs Ag/AgCl). The different applied potentials in this region have not dramatically changed the rate of hole transfer.[35] Any small differences in the hole transfer rate between the experiments at different potentials in Figure 3 do not correlate to the applied bias and are instead assigned as due to the relatively inhomogeneous nature of the sample. The activation energy for the hole transfer step to a water species on α-Fe_2O_3 is found to be the same, within the error of the measurement, at all potentials examined (0.42 ± 0.05 eV (245 mV), 0.48 ± 0.07 eV, (345 mV), 0.45 ± 0.04 eV (445 mV), 0.45 ± 0.05 eV (545 mV)), Figure 3. Significantly changing the applied bias is found to alter the yield of long-lived photoholes, and a decreased yield of surface-trapped holes is observed at lower potentials (Figure 4, 245 vs 445 mV). In all experiments the excitation intensity was kept constant; therefore the change in long-lived photohole yield is due to changes in the electron−hole recombination rate caused by a change in the background electron density of the films. Clearly the increased level of water oxidation at more positive potentials (Figure 1) is primarily due to decreased electron−hole recombination, providing more long-lived holes that are able to oxidize water, and not to a major change in the rate of the hole transfer step.

Temperature Dependence of Hole Kinetics on nc-TiO_2. Variable-temperature TAS experiments have also been carried out on a nc-TiO_2 photoanode. Previous TAS experiments have assigned the transient absorption centered at 460 nm to photoholes and an absorption that increases with wavelength to photoelectrons.[27] We have recently reported that photoholes on nc-TiO_2 photoanodes that are at potentials greater than the anodic photocurrent onset potential decay by two major pathways, fast electron−hole recombination and a slow hole transfer to water or to a surface-bound water species.[28] TAS decay traces of the photohole (460 nm) and photoelectron (900 nm)

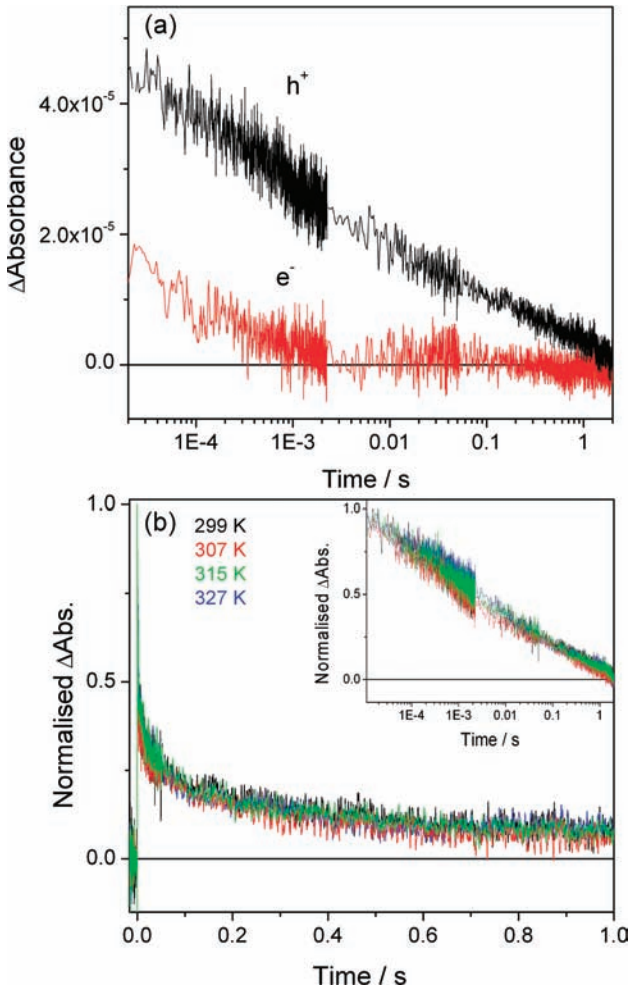

Figure 5. (a) TAS decay traces of the photohole (460 nm) and photoelectron (900 nm) at 299 K and (b) variable-temperature TAS decay traces recorded of the photohole (460 nm). TAS experiments were carried out following UV excitation (50 μJ cm^{-2}, 355 nm) of nc-TiO_2 held at 245 mV vs Ag/AgCl in 0.05 M NaOH/0.5 M $NaClO_4$.

recorded following the UV excitation of a positively biased nc-TiO_2 photoanode (245 mV vs Ag/AgCl, 355 nm 50 μJ cm^{-2} excitation, 0.05 M NaOH, 0.5 M $NaClO_4$) at 298 K are shown in Figure 5a. The electron signal has nearly completely decayed within 10 ms, indicating that the hole decay at times beyond this can be assigned to the hole transfer to water species, in agreement with our previous report.[28] No significant variation in the hole decay rate during the variable-temperature TAS experiment is observed (299−327 K), allowing us to conclude that the activation energy related to the hole reaction with water is either relatively small or zero, Figure 5b.

■ DISCUSSION

The balance between the rates of electron/hole recombination, electron transport and withdrawal, and the hole transfer from the metal oxide to solution controls the efficiency of the water splitting photoanodes, and a simplified kinetic model is shown in Scheme 1. This study and our previous results on nc-TiO_2 and α-Fe_2O_3 indicate that the decay of the very long-lived holes is the slowest, or rate-limiting, step in the PEC water splitting cell.[28,29] The hole signal studied on both species has been identified as being from surface-trapped holes,[25,27,29] and as such the terminal decay of this signal is likely to be associated with a terminal hole transfer step to a bound water species. Our TAS experiments cannot rule out the possibility that we are probing a slow hole transfer to another semiconductor-based trap site with a weak absorption in the UV/vis region; however the dependence of the hole decay rate and of the associated activation energies on the nature of the surface species being oxidized (methanol or water) does suggest that this is not the case.[29,36] Therefore we tentatively assign the rate-limiting step on both nc-TiO_2 and α-Fe_2O_3 to the terminal hole transfer step from the metal oxide to solution or to a surface-bound species.

Scheme 1 illustrates that increasing the rate of the terminal hole transfer (k_3) to levels that can effectively compete with electron−hole recombination (k_2) is one possible route to an increased quantum yield. Therefore improved routes to more efficient hole transfer to water or to adsorbed water are a key goal for material development. The rate of the terminal hole transfer is very slow on both materials studied, and this is despite both nc-TiO_2 and α-Fe_2O_3 having valence bands that lie at potentials (ca. +2.2 and +2.9 V vs NHE) significantly positive of the multielectron thermodynamic water oxidation potential (+1.23 V per electron); consequently any photoholes produced are expected to have ample oxidative power for water oxidation. It has been recently highlighted by Bard[37] that in the absence of a multielectron catalysis site we should instead consider the potentials for the one-electron oxidations of water such as for the oxidation of H_2O or OH^- to ·OH, which are significantly more positive (E^o = 2.38 and ca. 1.55 V, respectively) than the multielectron potentials.[38] Clearly the nature of the surface mechanism that occurs on nc-TiO_2 and α-Fe_2O_3 can greatly affect the thermodynamic driving force required, and any experimental data on this will aid our understanding of these materials.

On α-Fe_2O_3 we measure a significant activation energy to the terminal hole transfer step. The slow semiconductor liquid junction kinetics on α-Fe_2O_3 can, in part, at least be attributed to the presence of this thermal barrier. It has been proposed that, in part, the slow transfer of photoholes from α-Fe_2O_3 to water is due to the significant Fe(IV) character, and the direct measurement of the slow surface kinetics on α-Fe_2O_3 during these experiments is not in conflict with this proposal.[17] The addition of a water oxidation catalyst to the α-Fe_2O_3 surface is known to lower the onset potential of water oxidation and increase the overall efficiency of water splitting.[12,15,21] We have measured a significant activation energy to the hole reaction on Fe_2O_3, and the addition of a surface catalyst that provides a lower energy reaction route for the photoholes will lower the required photohole lifetime for water oxidation, which should in turn lead to a decreased requirement for a large anodic bias. On nc-TiO_2, a material with a significantly more positive valence band edge, which will produce more oxidizing photoholes, we do not observe a significant change in the photohole kinetics with temperature. If present, any activation energy for the photoholes on nc-TiO_2 is small, preventing its measurement. The lower activation energy on nc-TiO_2 correlates with the requirement of a reduced hole lifetime compared to α-Fe_2O_3 under similar conditions (~50 ms, cf. 3 s on α-Fe_2O_3).[28] The more positive valence band edge of nc-TiO_2 would be expected to lead to more strongly oxidizing photoholes on nc-TiO_2 than on α-Fe_2O_3, which would increase the driving force for the reaction on nc-TiO_2. To carry out a thermodynamic analysis, it would be necessary to correct for the effect of temperature on the

semiconductor band edges and the redox potentials in solution. Over the 25 K region examined, these are expected to be relatively small (approximately a 20 and 40 mV shift in surface potential for nc-TiO_2 and α-Fe_2O_3 respectively)[39] compared to the differences in our measured activation energy (~450 mV). It is interesting that the difference in the activation energies of the two materials is on the order of the difference in the valence band edges. We are currently examining a greater range of photoanodes to see if a clear trend in activation energies can be confirmed.

One of the key issues with nanostructured Fe_2O_3 electrodes has been the requirement of a relatively large anodic bias (~0.3−0.4 V vs the flat band potential) for water oxidation to occur. Therefore a motivation of this study was to examine any relation between the photoelectrode potential and the kinetics and the thermodynamics of the hole during the water oxidation. We have examined the photohole dynamics at four different potentials that are significantly positive on Fe_2O_3. The activation energies obtained for this rate-limiting step are the same within the experimental error at all four potentials. The very slight differences in the rate of the hole reaction at the different potentials (Figure 3) are not significant enough to account for the large change in the photocurrent yield; the magnitude of the photocurrent at 245 mV on Fe_2O_3 was ~65% of that recorded at 445 mV vs Ag/AgCl under Xe lamp illumination, Figure 1. Therefore we conclude that at potentials significantly positive of the photocurrent onset the application of a more positive bias does not markedly change the oxidative power of the trapped holes on APCVD α-Fe_2O_3. It has been reported that applying a positive bias lowers the level of electron−hole recombination,[29] and we do observe a significantly higher population of long-lived photoholes at the higher biases examined (Figure 4), which gives rise to the higher photocurrents. The requirement of a relatively large anodic bias (~0.4 V) is at least in part due to the need to produce very long-lived holes. These findings are in good agreement with our previous report on nc-TiO_2, which showed that changing the potential of the nc-TiO_2 film did not dramatically alter the rate of water oxidation and that the primary role was to alter the level of electron−hole recombination.[28] The change in concentration of surface-trapped holes with applied potential may lead to slight differences in the average energy of the trapped photoholes if the trap states occur at a distribution of different energies; however we are not able to detect this relatively small change.

Although we have tentatively assigned the rate-limiting step in our PEC water splitting cell to a hole transfer to solution or to an adsorbed water species, the chemical nature of this step is not clear. The surface oxidation of water on both nc-TiO_2 and α-Fe_2O_3 is a multihole reaction that must occur via several steps. A set of multistep hole reactions that involve the buildup of surface intermediates might be expected to have a rate that is dependent on the concentration of long-lived photoholes. We did not see any clear evidence of the hole reaction rate on α-Fe_2O_3 being dependent on the concentration of long-lived holes; however it is difficult to rule out that we are not operating under conditions where we already have multiple holes at a single reaction site on α-Fe_2O_3. Our TAS experiments involve the averaging of large numbers of consecutive laser shots, and it is not clear if we are probing one distinct step or the averaged signal of a multistep process. In order to look for multistep processes, we have performed single-shot analyses of the TAS decay traces on nc-TiO_2 (detailed in the Supporting Information). These analyses show that any differences in the photohole decay rate are very small, and the change in the amplitude of the hole signal at 100 ms between laser shots is less than ±6%.[40] This is consistent with a hole reaction on nc-TiO_2 that proceeds via a series of indistinguishable, or common, intermediates. The oxidation of surface OH^- groups has been proposed to be a common step in the water oxidation reaction on this material, and our data are consistent with this as one possible interpretation. It is clear that to definitively assign the mechanism occurring, a transient measurement that directly probes the surface chemical functionality under operating conditions will be required.

CONCLUSIONS

In this paper we have used TAS to investigate the slow hole reaction kinetics during light-driven water oxidation on two nanostrucutured metal oxides, α-Fe_2O_3 and nc-TiO_2, in a complete PEC cell. The requirement of very long-lived photoholes on α-Fe_2O_3 for water splitting to occur correlates with the presence of a significant thermal barrier to the surface hole reaction. This is in contrast to nc-TiO_2, a material with a more positive valence band edge, where the photohole dynamics are faster and are not strongly temperature dependent. We have examined the photohole kinetics on α-Fe_2O_3 at four different potentials and found that the difference in water oxidation reactivity between the potentials is due to a change in the yield of long-lived photoholes and not due to a major change in the reactivity of the long-lived photoholes.

ASSOCIATED CONTENT

Supporting Information. Details of transient photocurrent measurements on α-Fe_2O_3; UV/vis spectra of the photocatalysts and details of the single-shot analysis of the TAS data. This material is available free of charge via the Internet at http://pubs.acs.org.

AUTHOR INFORMATION

Corresponding Author
d.klug@imperial.ac.uk

ACKNOWLEDGMENT

We are grateful to Dr. W. Leng for his useful insights and Ms. Xiaoe Li for assistance in TiO_2 paste preparation. The work at Imperial College London was funded by the EPSRC. K.S. and M.G. thank the Swiss National Energy Office for financial support under the PEC House project.

REFERENCES

(1) Boddy, P. J. *J. Electrochem. Soc.* **1968**, *115*, 199–203.
(2) Fujishima, A.; Honda, K. *Nature* **1972**, *238*, 37.
(3) Kudo, A.; Miseki, Y. *Chem. Soc. Rev.* **2009**, *38*, 253–278.
(4) Osterloh, F. E. *Chem. Mater.* **2008**, *20*, 35–54.
(5) Bard, A. J.; Fox, M. A. *Acc. Chem. Res.* **1995**, *28*, 141–145.
(6) Bak, T.; Nowotny, J.; Rekas, M.; Sorrell, C. C. *Int. J. Hydrogen Energy* **2002**, *27*, 991–1022.
(7) Asahi, R.; Morikawa, T.; Ohwaki, T.; Aoki, K.; Taga, Y. *Science* **2001**, *293*, 269–271.
(8) Khan, S. U. M.; Al-Shahry, M.; Ingler, W. B. *Science* **2002**, *297*, 2243–2245.

(9) Wang, Y.; Meng, Y.; Ding, H.; Shan, Y.; Zhao, X. *J. Phys. Chem. C* **2008**, *112*, 6620–6626.
(10) Durrant, J.; Haque, S.; Palomares, E. *Coord. Chem. Rev.* **2004**, *248*, 1247–1257.
(11) Peter, L. *Acc. Chem. Res.* **2009**, *42*, 1839–1847.
(12) Kay, A.; Cesar, I.; Gratzel, M. *J. Am. Chem. Soc.* **2006**, *128*, 15714–15721.
(13) Gratzel, M. *Nature* **2001**, *414*, 338–344.
(14) Cesar, I.; Sivula, K.; Kay, A.; Zboril, R.; Graetzel, M. *J. Phys. Chem. C* **2009**, *113*, 772–782.
(15) Tilley, S.; Cornuz, M.; Sivula, K.; Gratzel, M. *Angew. Chem., Int. Ed.* **2010**, *49*, 6405–6408.
(16) Gardner, R. F. G.; Sweett, F.; Tannder, D. *J. Phys. Chem. Solids* **1963**, *24*, 1183–1186.
(17) Dare-Edwards, M. P.; Goodenough, J. B.; Hamnett, A.; Trevellick, P. R. *J. Chem. Soc., Faraday Trans. 1* **1983**, *79*, 2027–2041.
(18) Kennedy, J. H.; Frese, K. W. *J. Electrochem. Soc.* **1978**, *125*, 709–714.
(19) Mohapatra, S.; John, S.; Banerjee, S.; Misra, M. *Chem. Mater.* **2009**, *21*, 3048–3055.
(20) Duret, A.; Gratzel, M. *J. Phys. Chem. B* **2005**, *109*, 17184–17191.
(21) Zhong, D.; Gamelin, D. *J. Am. Chem. Soc.* **2010**, *132*, 4202–4207.
(22) Yang, X. J.; Tamai, N. *Phys. Chem. Chem. Phys.* **2001**, *3*, 3393–3398.
(23) Tamaki, Y.; Furube, A.; Murai, M.; Hara, K.; Katoh, R.; Tachiya, M. *Phys. Chem. Chem. Phys.* **2007**, *9*, 1453–1460.
(24) Bahnemann, D.; Henglein, A.; Lilie, J.; Spanhel, L. *J. Phys. Chem.* **1984**, *88*, 709–711.
(25) Yoshihara, T.; Katoh, R.; Furube, A.; Tamaki, Y.; Murai, M.; Hara, K.; Murata, S.; Arakawa, H.; Tachiya, M. *J. Phys. Chem. B* **2004**, *108*, 3817–3823.
(26) Yoshihara, T.; Tamaki, Y.; Furube, A.; Murai, M.; Hara, K.; Katoh, R. *Chem. Phys. Lett.* **2007**, *438*, 268–273.
(27) Tang, J. W.; Durrant, J. R.; Klug, D. R. *J. Am. Chem. Soc.* **2008**, *130*, 13885–13891.
(28) Cowan, A. J.; Tang, J. W.; Leng, W. H.; Durrant, J. R.; Klug, D. R. *J. Phys. Chem. C* **2010**, *114*, 4208–4214.
(29) Pendlebury, S.; Barroso, M.; Cowan, A. J.; Sivula, K.; Tang, J.; Gratzel, M.; Klug, D. R.; Durrant, J. R. *Chem. Commun.* **2011**, *47*, 716–718.
(30) Xiao-e, L.; Green, A. N.; Haque, S. A.; Mills, A.; Durrant, J. R. *J. Photochem. Photobiol., A* **2004**, *162*, 253–259.
(31) Sawyer, D. T.; Sobkowiak, A.; Roberts, J. L. *Electrochemistry for Chemists*, 2nd ed.; Wiley-Interscience: New York, 1995.
(32) Wrighton, M. S.; Ginley, D. S.; Wolczanski, P. T.; Ellis, A. B.; Morse, D. L.; Linz, A. *Proc. Natl. Acad. Sci. U. S. A.* **1975**, *72*, 1518–1522.
(33) Glasscock, J.; Barnes, P.; Plumb, I.; Savvides, N. J. *Phys. Chem. C* **2007**, *111*, 16477–16488.
(34) Miller, E.; Paluselli, D.; Marsen, B.; Rocheleau, R. *Thin Solid Films* **2004**, *466*, 307–313.
(35) We do not rule out a small change in the hole reaction rate; however any differences are very small compared to the change in the magnitude of the long-lived hole signal between the two potentials examined. A detailed TAS study on the dynamics of the charge carriers on Fe_2O_3 at a greater range of different potentials is currently under way.
(36) Tamaki, Y.; Furube, A.; Murai, M.; Hara, K.; Katoh, R.; Tachiya, M. *J. Am. Chem. Soc.* **2006**, *128*, 416–417.
(37) Bard, A. J. *J. Am. Chem. Soc.* **2010**, *132*, 7559–7567.
(38) Bard, A. J.; Parsons, R. *Standard Potentials in Aqueous Solution*; IUPAC: New York, 1985.
(39) Fokkink, L. G. J.; Dekeizer, A.; Lyklema, J. *J. Colloid Interface Sci.* **1989**, *127*, 116–131.
(40) A maximum deviation of ±6% in the component of the hole trace assigned to the terminal hole transfer step is observed. The details of this experiment are outlined in the Supporting Information.